

Tuning the Glass Transition of and Ion Transport within Hydrogen-Bonded Layer-by-Layer Assemblies

Jodie L. Lutkenhaus,[†] Kathleen McEnnis, and Paula T. Hammond*

Department of Chemical Engineering, Massachusetts Institute of Technology, 77 Massachusetts Avenue
66-546, Cambridge, Massachusetts 02139

Received June 19, 2007; Revised Manuscript Received August 6, 2007

ABSTRACT: The influence of pH and ionic strength on the structure and properties of hydrogen-bonded layer-by-layer (LbL) assemblies of poly(ethylene oxide) (PEO) and poly(acrylic acid) (PAA) is explored. The degree of inter- and intramolecular hydrogen bonding is estimated from Fourier-transform infrared spectroscopy, the glass transition temperature is measured using differential scanning calorimetry of bulk free-standing films, and ionic conductivity is studied using electrochemical impedance spectroscopy. Results indicate that (PEO/PAA) LbL films assembled without added salt are sensitive to pH, with a T_g decrease (59–26 °C) and intermolecular hydrogen bonding increase (27 to 51% COOH groups bonding with PEO) with increasing assembly pH (2 to 3). Films assembled in the presence of 0.1 M lithium triflate exhibit properties independent of assembly pH ($T_g \sim 48$ °C and 12% COOH groups bonding with PEO), presumably due to the “screening” of hydrogen bonds. Ionic conductivity is found to range from 10^{-6} to 10^{-10} S cm⁻¹, depending on humidity, plasticization, and salt content.

Introduction

Hydrogen bonding between two macromolecular species gives rise to a breadth of interesting superstructures observed in nature, interpolymer complexes,^{1–3} and layer-by-layer assemblies.^{4–7} While hydrogen-bonding interactions between a proton-accepting and a proton-donating monomer may be small (~ 2 – 10 kcal/mol), the sum of these interactions, from the association of polymeric species, is sufficient to produce a stable complex.⁸ A simple and easy means of creating stable hydrogen-bonded thin films is the layer-by-layer (LbL) assembly technique, where a substrate (e.g., silicon, PTFE, ITO) is alternately exposed to aqueous solutions of proton-donating and -accepting polymers.^{4–7} In general, these thin films appear to behave as miscible blends, where each “layer” of deposition produces an interdigitated morphology,^{9–11} yielding properties similar to solution-cast complexes.

Hydrogen-bonded LbL multilayers of proton-donor poly(acrylic acid) (PAA) or poly(methacrylic acid) (PMAA) and complementary proton-acceptor poly(ethylene oxide) (PEO) have been recently explored as solid polymer electrolytes, drug delivery vehicles, and responsive capsules.^{12–15} To create stable hydrogen-bonded films (20–90 nm thickness per layer pair), an acidic assembly pH is required to suppress the ionization of the poly(carboxylic acid), and above a critical pH, film assembly is unfavorable owing to negative electrostatic repulsion (pH = 3.6 for PEO/PAA and pH = 4.5 for PEO/PMAA).¹² Conversely, a stable LbL film may be “erased” when the solution pH is greater than the critical pH.^{13,16} Other reports of hydrogen bond destabilization within multilayer films detail the creation of a microporous morphology.^{17–19}

The marked stability of these films in the dry state led to the investigation of (PEO/PAA) multilayers in electrochemical devices as solid polymer electrolytes. DeLongchamp et al.¹² proposed that lithium-doped hydrogen-bonded LbL films containing PEO might possess room-temperature conductivities

approaching amorphous PEO–LiTriflate ($\sim 10^{-6}$ S cm⁻¹),^{20,21} given that hydrogen-bonding interactions suppress PEO crystallization. A single assembly pH was investigated, and the reported dry conductivities of the LbL assemblies (7% relative humidity (RH), 25 °C), even when doped with lithium triflate, were $\sim 10^{-10}$ S cm⁻¹.¹² The reason for the discrepancy was not well understood at that time, but some hypotheses¹² were suggested: (i) a high glass transition temperature, leading to a “glassy” matrix and low charge carrier mobility, (ii) a high cross-link density, decreasing segmental motion, and (iii) low PEO content, where PAA dilutes ion-conducting PEO. However, at that time little was known of the composition, structure, and materials properties of the adsorbed multilayers because film isolation proved challenging.

Recently, the authors reported a nondestructive “peel-away” technique,¹⁰ for successfully isolating hydrogen-bonded LbL films of sufficient mass (> 20 mg) and area (> 4 in²) to study the glass transition temperature, modulus, and dynamic mechanical response of “neat” (without lithium salt) (PEO/PAA) multilayers.¹⁰ Of note, PEO crystallization was suppressed, and a single glass transition temperature (T_g) that varied with assembly pH was reported. The T_g –pH dependency was proposed to be related to the intra- and intermolecular hydrogen bonding of PAA.¹⁰ A more recent report²² investigates the effect of hydrophobic interactions within multilayers of PAA and hydrophobically modified PEO, where alkyl groups end-capped the PEO chain. In these previous studies, the influence of salt addition upon materials properties and pH-dependency of (PEO/PAA) films was not explored. This understanding is critical for the design of LbL electrolytes with sufficient charge carrier concentrations for electrochemical applications.

Here, we examine and estimate the degree of intra- and intermolecular hydrogen bonding of PAA within hydrogen-bonded (PEO/PAA) multilayers assembled at varying pH and ionic strength. Films assembled in the presence of 0.1 M lithium triflate are compared to those assembled without, and the resulting properties (e.g., glass transition temperature, ionic conductivity) are found to be quite unique. The presence of added salt appears to encourage dimerization of PAA and

* Corresponding author. E-mail: hammond@mit.edu.

[†] Current address: Department of Chemical Engineering, Yale University, New Haven, CT.

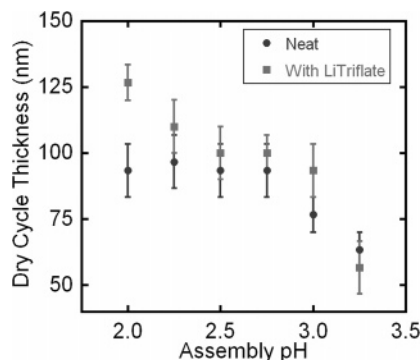


Figure 1. Dry cycle thickness of neat (PEO/PAA) and (PEO/PAA)_{LiTrif} multilayers on silicon with varying assembly pH 2.00 to 3.25. Total thickness was measured using profilometry and averaged over a sample 30 layer pairs thick.

weaken PEO–PAA interactions, yielding PAA-rich films with an elevated glass transition temperature. Additionally, when assembly pH was varied, a maximum dry ionic conductivity of lithium triflate-doped films (assembly pH 3.0) was observed, $\sim 10^{-8}$ S cm⁻¹ (0% RH, 35 °C). These results support the previously proposed hypothesis regarding the pH dependency of intra- and intermolecular hydrogen bonding of PAA,¹⁰ where the two interactions compete within neat (PEO/PAA) multilayers. Also, findings from FTIR spectroscopy, differential scanning calorimetry (DSC), and electrochemical impedance spectroscopy (EIS) are compared to reports of solution-cast PEO/PAA complexes.

Results and Discussion

Multilayer Growth. The layer-pair, or cycle, thickness for LbL systems varies widely depending on the type of system chosen.^{12,23,24} Previous work by DeLongchamp et al.¹² indicated that modest addition of salt (<0.5 M LiCF₃SO₃) enhances the cycle thickness of hydrogen-bonded multilayers of PEO and PAA, an effect attributed to screening-enhanced adsorption;¹² however, this phenomenon was only investigated at a single assembly pH, 2.5. In this case, the layer-pair thickness may be interpreted as an indicator of the strength of intermolecular interaction, where weaker interactions between polymers A and B result in thicker, lightly cross-linked (A/B) LbL films.^{12,23,24}

To understand the effect of added salt and assembly pH upon the layer-pair thickness in hydrogen-bonded LbL assemblies, two systems were investigated: neat (PEO/PAA) and (PEO/PAA)_{LiTrif}, where “neat” (PEO/PAA) refers to films assembled in the absence of added salt and (PEO/PAA)_{LiTrif} refers to films assembled in baths containing 0.1 M LiCF₃SO₃, lithium triflate. The thickness of the dry LbL films, 30 layer pairs each, assembled at varying pH was measured using profilometry, and the cycle thickness was calculated by simply dividing total film thickness by the number of cycles (Figure 1). Observed neat (PEO/PAA) layer-pair thicknesses coincided with those earlier reported,¹² where cycle thickness was 80–90 nm from pH 2 to 2.75 and decreased to 60 nm per cycle at assembly pH 3.25. This decrease results from the partial ionization of PAA at higher pH, yielding a “modulation window” where film formation is hindered by electrostatic repulsion.¹² In contrast, (PEO/PAA)_{LiTrif} multilayers were generally thicker than their neat counterparts, and cycle thickness decreased from 126 to 50 nm at assembly pH 2.00 to 3.25, where a modulation window was also observed. The presence of this effect suggests that the ionization of PAA ($pK_a = 5.5\text{--}6.5$),^{2,25} even in the presence of 0.1 M salt, is sufficiently strong so as to suppress film formation at elevated pH > 3.

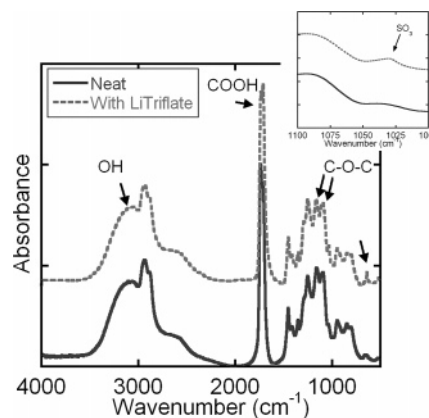


Figure 2. Sample FTIR spectra of neat (PEO/PAA) and (PEO/PAA)_{LiTrif} multilayers assembled at pH 3 on IR-transparent silicon. Both spectra show evidence of PEO, PAA, and hydrogen-bonding interactions. Inset is of the SO₃ region, ~ 1040 cm⁻¹.

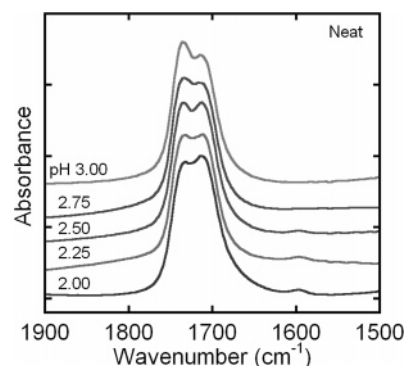


Figure 3. FTIR spectra of the carboxylic acid region of neat (PEO/PAA) multilayers assembled at pH 2.00–3.00 on IR-transparent silicon. The two peaks (~ 1710 and 1740 cm⁻¹) appear to decrease and increase in intensity, respectively, as assembly pH increases.

The difference in cycle thickness between neat (PEO/PAA) and (PEO/PAA)_{LiTrif} systems suggests that the nature of intermolecular hydrogen bonding between PEO and PAA changes in the presence of added salt. The presence of 0.1 M salt results in thicker films because intermolecular hydrogen bonding may be effectively shielded, or weakened, leading to chain conformations containing many loops and tails. Also, any COO⁻ functional groups present at these conditions may be shielded in the presence of lithium triflate.

FTIR Spectroscopy Analysis. To further understand the structural state of PAA and PEO within the LbL film, Fourier-transform infrared (FTIR) spectra of neat (PEO/PAA) and (PEO/PAA)_{LiTrif} multilayers in dry nitrogen were collected for films assembled at pH ranging from 2 to 3. Sample spectra of films assembled at pH 3 are shown in Figure 2; here, the presence of PEO and PAA is clear in both systems. Peak positions at 850, 1060–1120, and 1120–1170 cm⁻¹ are similar to C–O–C stretch and CH₂ rock peaks reported for PEO in its amorphous state (855, 1107, and 1140 cm⁻¹).²⁶ Also, strong absorption at 1700–1750 cm⁻¹ is indicative of carbonyl C=O stretching^{27–29} typical of poly(carboxylic acid)s such as PAA, and evidence of hydroxyl–hydrogen bonding is demonstrated by the broad absorption peak, ~ 3100 cm⁻¹.^{30,31} Films assembled in the presence of LiCF₃SO₃ exhibited increased absorbance near 1040 cm⁻¹ attributed to SO₃ (Figure 2 inset),^{29,32} suggesting that some amount of lithium triflate is incorporated within the (PEO/PAA)_{LiTrif} film.

The carboxylic acid region, which is $\sim 1700\text{--}1750$ cm⁻¹ for COOH and ~ 1550 cm⁻¹ for COO⁻,^{13,27–29} was of particular

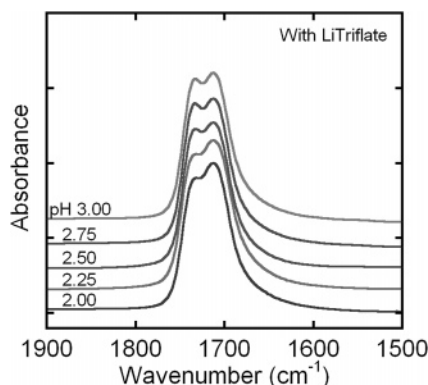


Figure 4. FTIR spectra of the carboxylic acid region of (PEO/PAA)_{LiTrif} multilayers assembled at pH 2.00–3.00 on IR-transparent silicon. Peaks locations (~ 1714 and 1740 cm^{-1}) and intensity appear to be relatively invariant despite increasing assembly pH.

interest because it describes the state of PAA within the LbL film. Figure 3 presents a peak with two features (~ 1710 and $\sim 1740\text{ cm}^{-1}$) that was observed in neat (PEO/PAA) systems. Given the work of Coleman and Painter et al.,^{31,33,34} the lower-wavenumber peak ($\sim 1710\text{ cm}^{-1}$) is attributed to the intramolecular hydrogen bonding of PAA, where two carboxylic acid groups form a dimer. The higher-wavenumber peak ($\sim 1740\text{ cm}^{-1}$),^{31,34} associated with intermolecular hydrogen bonding, can be attributed to acid–ether interactions between PAA and PEO. The position of the two peaks remained constant at $1711\text{--}1713$ and $1739\text{--}1740\text{ cm}^{-1}$ with assembly pH. Qualitatively, the 1711 cm^{-1} peak intensity appears to decrease relative to 1740 cm^{-1} intensity as assembly pH increases. A weak, broad peak near 1600 cm^{-1} is present for samples prepared at pH 2.50, 2.25, and 2.00, but the meaning of this phenomenon is unclear. Also of note, a $\text{Li}^+\text{--COO}^-$ peak ($\sim 1550\text{--}1570\text{ cm}^{-1}$, broad and strong)^{28,35} was not observed in either of the investigated (PEO/PAA) systems.

Films of (PEO/PAA)_{LiTrif} were characterized in a similar manner. Spectra in the COOH region (Figure 4) exhibit a similar shape to those observed in the neat (PEO/PAA) system (Figure 3). Here, too, a peak with two features positioned at $1714\text{--}1715$ and $1739\text{--}1741\text{ cm}^{-1}$ was observed. Qualitatively, the $\sim 1715\text{ cm}^{-1}$ peak intensity decreased only slightly with respect to the $\sim 1739\text{ cm}^{-1}$ peak intensity as assembly pH increased.

Assuming the observed peaks may be modeled as the summation of two Gaussian curves, each contribution may be separately estimated (Figure 1 of the Supporting Information). From the calculated area of each Gaussian contribution, the percentage of COOH groups participating in intermolecular hydrogen bonding (or “free” COOH) (Figure 5) is calculated using the following relationship from Coleman et al.:³¹ intermolecular H-bonding COOH = $\text{area}_{1740}/(\text{area}_{1711}/a_r + \text{area}_{1740})$. In this case, the absorptivity ratio, a_r , was assumed to be similar to Coleman’s value reported for methacrylic acid copolymer (EMAA)/polyether blends (EPO) ($a_r = 1.6$).³¹ For the neat (PEO/PAA) system, the percentage of COOH groups participating in intermolecular hydrogen bonding increases (27 to 51%) with increasing assembly pH (2 to 3, respectively); on the other hand, for the (PEO/PAA)_{LiTrif} system, 12–15% of COOH groups participate in intermolecular hydrogen bonding, independent of assembly pH. For comparison in neat PMAA/PEO LbL films (assembled at pH 2), Sukhishvili and Granick¹³ estimate that 10% of carboxylic acid groups are intermolecularly hydrogen-bonded, though it should be noted that these measurements were performed in D₂O. Possible error in the analysis may arise from the assumed absorptivity coefficient, which may

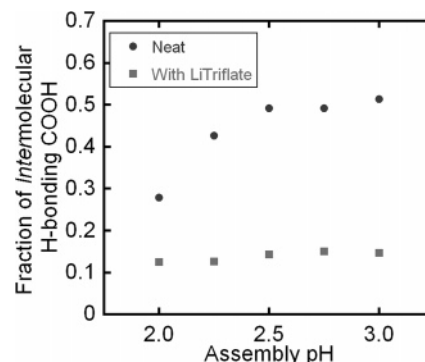


Figure 5. Fraction of intermolecular H-bonding PAA monomers, as calculated using ref 33, for (PEO/PAA) and (PEO/PAA)_{LiTrif} multilayers. Intermolecular H-bonding COOH = $\text{area}_{1740}/(\text{area}_{1711}/a_r + \text{area}_{1740})$.³¹ The areas were calculated assuming the summation of two Gaussian peaks, as described in the text. The absorptivity coefficient used in these calculations was that of an EMAA/EPO blend,³¹ which may introduce error as described within the text.

not be identically $a_r = 1.6$ (EMAA/EPO blend)³¹ for this particular system (PEO/PAA LbL film). The absorptivity coefficient of PEO/PAA is unknown.

This analysis suggests that the addition of lithium triflate to each dipping bath promotes intramolecular hydrogen bonding of PAA, which may explain the observed cycle thicknesses discussed previously. (PEO/PAA)_{LiTrif} multilayers exhibited greater cycle thicknesses, which points to weaker intermolecular hydrogen-bonding interactions relative to neat (PEO/PAA) systems. From FTIR, the degree of intermolecular interaction was estimated, where films with added salt have significantly less (12–15% intermolecular H-bonding COOH) PEO–PAA hydrogen bonding as compared to neat (PEO/PAA) multilayers (27–51% intermolecular H-bonding COOH, depending on pH). This hypothesis suggests that inter- and intramolecular interactions compete during film formation, where added salt “screens” PEO–PAA hydrogen bonding regardless of assembly pH. Though FTIR spectroscopy yields information concerning the extent of hydrogen bonding of PAA monomer units, the overall cross-link density of the multilayer systems is unknown because the fraction of PEO monomer units participating in hydrogen bonding could not be quantified using this analysis.

For comparison, solution-cast blends of PEG and PAA with no added salt both demonstrated intra- and intermolecular hydrogen bonding via FTIR spectroscopy (1706 and 1732 cm^{-1} , respectively),²⁸ where the addition of PEG was shown to disrupt cyclic dimers and to favor the formation of acid–ether hydrogen bonding.

Of note, PAA in electrostatically assembled LbL films is known to further ionize within the film, as PAA pK_a decreases to accommodate electrostatic cross-linking with polyamines,^{24,25} however, in hydrogen-bonding systems, the ionization of PAA within the film is unfavorable, as it may compromise film stability.^{13,16} From FTIR, the absence of the COO^- band ($\sim 1550\text{ cm}^{-1}$) in both (PEO/PAA) systems indicates that PAA is present in its fully protonated form and is capable of hydrogen bonding with PEO. To disrupt (PEO/PAA) multilayer stability, exposing the as-made LbL film to water at pH > 3.6 results in complete deconstruction, where PAA is 2–3% ionized.¹³ When ionic strength is increased, this critical pH of deconstruction increases (i.e., stability increases) because added salts appear to screen the ionized PAA.^{13,16} The onset of pH stability for this system is similar to those reported for solution complexes of PEO and PAA.^{26,36}

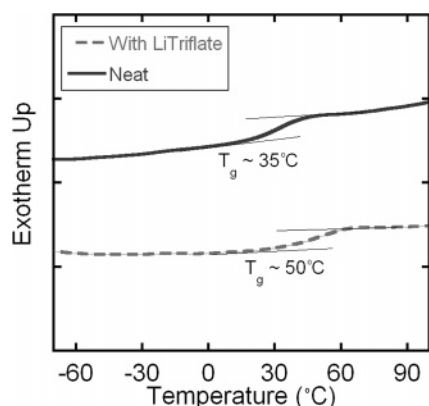


Figure 6. DSC trace (second heating scan) for 100 layer pairs (~ 8 μm thick) of neat (PEO/PAA) and (PEO/PAA)LiTrif multilayers assembled at pH 2.75. Both films exhibit a single glass transition, and the T_g is estimated from the inflection point of the sigmoidal region. The melting peak of neat PEO, ~ 65 $^{\circ}\text{C}$, is absent in LbL films.

Thermal Properties and Composition. Given varying degrees of acid–ether hydrogen bonding, as evidenced above, the glass transition temperature and composition of PEO/PAA multilayers are expected to reflect these interactions. The thermal properties of neat (PEO/PAA) and (PEO/PAA)_{LiTrif} films assembled at pH 2 to pH 3.25 were investigated using DSC. LbL films (100 layer pairs ranging from 6 to 10 μm thick) were assembled atop a polystyrene substrate, peeled away, and used for analysis. Samples were cooled to -90 $^{\circ}\text{C}$, heated to 105 $^{\circ}\text{C}$ at 10 $^{\circ}\text{C}/\text{min}$, held at 105 $^{\circ}\text{C}$ for 5 min, and cooled back to -90 $^{\circ}\text{C}$ at the same rate. This procedure was repeated for three thermal cycles. During the first heating cycle, a glass transition was observed followed by a broad endothermic peak attributed to the desorption or evaporation of water (2–3 wt % water from TGA); second and third scans both yielded identical scans with a single glass transition at a temperature above the first cycle's T_g , and the endothermic peak observed in the first heating scan was absent (Figure 2 of the Supporting Information). Data and analysis presented here apply to behavior observed during the second heating cycle.

A typical thermal response from DSC for both neat (PEO/PAA) and (PEO/PAA)_{LiTrif} LbL assemblies is shown in Figure 6. In the temperature range investigated, both LbL systems (assembled at pH 2.75) exhibit a single glass transition temperature (35 and 50 $^{\circ}\text{C}$ for neat (PEO/PAA) and (PEO/PAA)_{LiTrif} multilayers, respectively). A melting peak for PEO (65 $^{\circ}\text{C}$) was not observed in either LbL system.

Because the thermal trace of (PEO/PAA)_{LiTrif} LbL assemblies appears similar to that of neat (PEO/PAA) multilayers, previous findings¹⁰ may be extended to this new system. The absence of a melting peak suggests that PEO within the film is amorphous, rather than crystalline. Also, the presence of a single glass transition temperature (50 $^{\circ}\text{C}$, (PEO/PAA)_{LiTrif} assembled at pH 2.75) indicates that this LbL film, consisting of PEO, PAA, and lithium triflate, behaves as a miscible blend. For comparison, the observed T_g of PEO (MW = 4×10^6) and PAA (MW = 90 000) is -56 and 99 $^{\circ}\text{C}$, respectively.¹⁰ Further evidence of miscibility was given by the clear, transparent appearance of the film. Observed changes in the glass transition temperature are indicative of corresponding changes in PEO content, which decreases in films assembled in the presence of ionic strength.

Similar results have also been observed for solution-cast blends of PEG and PAA, where these hydrogen-bonded blends, miscible over the entire composition range, exhibited a T_g that was composition-dependent and intermediate between those of the pure constituent polymers.^{28,37}

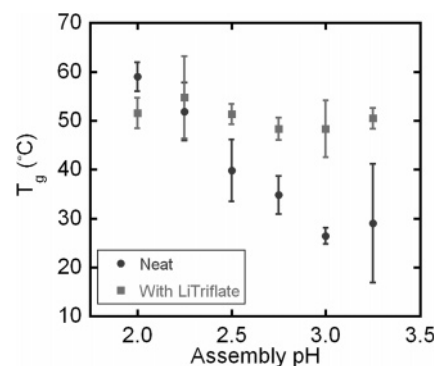


Figure 7. Variation of glass transition temperature with assembly pH. The (PEO/PAA)_{LiTrif} system exhibits a T_g that is invariant with assembly pH, whereas the T_g of the neat (PEO/PAA) system decreases with increasing pH. The T_g is estimated from the second heating scan.

When LbL assembly pH varies from pH 2 to pH 3.25, the glass transition temperature of the neat and the lithium triflate systems each vary in a different manner (Figure 7). Neat (PEO/PAA) multilayers exhibit a T_g that decreases with increasing pH (59 $^{\circ}\text{C}$ at assembly pH 2 and 26 $^{\circ}\text{C}$ at pH 3), as previously described;¹⁰ however, (PEO/PAA)_{LiTrif} multilayers exhibit a T_g (48–54 $^{\circ}\text{C}$) that is relatively invariant of assembly pH. Of note, the T_g of neat (PEO/PAA) multilayers assembled at pH 3.25 varied widely, as shown by the breadth of the error bar in Figure 7, likely a result of the film's instability at this condition. In some samples, two glass transition temperatures were observed for neat (PEO/PAA) systems assembled at pH 3.25, which suggests some degree of phase separation at this condition. These films also exhibited an opaque appearance, and optical microscopy demonstrated phase separation within the film on the micrometer scale.

The behavior of the T_g of neat (PEO/PAA) multilayers is believed to be caused by the tendency of PAA to intramolecularly hydrogen bond.¹⁰ For instance at pH 2, much of the carboxylic acid functional groups are occupied via intramolecular hydrogen bonding (or dimer formation), and few COOH groups are available for intermolecular hydrogen bonding with PEO. Recall that at assembly pH 2 FTIR results indicated that 27% of PAA units participate in hydrogen bonding with PEO. To compensate for the lack of “free” PAA acid groups (i.e., COOH groups H-bonding with PEO), the film will be enriched with PAA and the glass transition temperature will shift toward that of PAA (99 $^{\circ}\text{C}$). As assembly pH increases from 2.00 to 3.25, intermolecular hydrogen bonding becomes more favorable relative to intramolecular hydrogen bonding: the amount of PEO within the film increases and T_g decreases. For example, at assembly pH 3, the fraction of PAA units hydrogen bonding with PEO increases to 51%, and T_g decreases to 26 $^{\circ}\text{C}$. Though PEO was once thought to be the dominant component in PEO/PAA LbL films,¹² the observed glass transition temperature reflects a miscible blend that is rich in PAA.

When lithium triflate is present in each assembly bath, the multilayers' glass transition temperature remains constant with respect to assembly pH (Figure 7), but the reason for this behavior is not well understood. We believe that the conformation of each polymer in 0.1 M LiCF₃SO₃ solution may play a key role. PAA in a solution of moderate ionic strength may be sufficiently shielded such that intramolecular hydrogen bonding is promoted. At such high ionic strength, the solution structure of PAA is highly shielded (coiled sphere)³⁸ and may not change appreciably in the pH range investigated. In a similar solution environment, the hydrodynamic radius of PEO will decrease

with increasing ionic strength but will remain constant with changes in solution pH.²⁶ The presence of lithium cations, which can interact with EO units via ion-dipole forces, may compete with PEO–PAA intermolecular hydrogen bonding, thus “shielding” the hydrogen-bonding interaction. Even when the assembly pH is varied (in 0.1 M LiCF₃SO₃), this “shielding” appears to consistently inhibit PEO–PAA intermolecular interactions, noted in FTIR spectroscopy studies (Figure 5). (PEO/PAA)_{LiTrif} assemblies exhibited COOH spectra and intermolecular hydrogen bonding (12–15%) that remained relatively constant despite variation in assembly pH. Also, recall that from FTIR spectroscopy COOH is fully protonated and no ionization (COO[−]) was observed.

From observed variations in T_g , one might expect a similar response in film composition. The Fox equation may be used to roughly estimate film composition, assuming an ideal polymer blend with no interactions;³⁹ however, the presence of hydrogen bonding constitutes a molecular interaction that may cause deviation from ideality.⁴⁰ For this reason, the detection of composition via elemental analysis was attempted.

LbL films were analyzed for carbon, hydrogen, and oxygen content, but results appear inconclusive. For changes in neat PEO/PAA multilayer composition, carbon, hydrogen, and oxygen content is expected to vary from 50.0, 5.6, and 44.4% (pure PAA) to 54.5, 9.1, and 36.4% (pure PEO), respectively. From the Fox equation, it is estimated that the composition of neat (PEO/PAA) films assembled at pH 2.00 and pH 3.00 to be 25 and 46 mol % PEO, respectively. Also, the carbon, hydrogen, and oxygen content in this pH range is expected to vary from 50.8 to 51.5, 6.2 to 6.8, and 43.1 to 41.7 wt %, respectively. Unfortunately, analysis error (± 0.3 wt %) exceeded the projected variation in composition. For example, neat (PEO/PAA) multilayers assembled at pH 2.5 gave a composition of 51.2% carbon, 6.7% hydrogen, and 42.2% oxygen, which corresponds to a composition of $45 \pm \text{wt } \%$ PEO based upon hydrogen content and accounting for 0.3 wt %. Multilayer film composition calculated from elemental analysis for both systems is summarized in Figure 3 of the Supporting Information. Overall, PEO content within (PEO/PAA) LbL films detected using elemental analysis ranges from 28 to 50 wt % PEO. For solution-blends of PEO and PAA, isolated precipitate was reported to be 52 wt % (64 mol %) PEO without pH adjustment³⁷ or 35–45 wt % (25–33 mol %) PEO when pH < 4.³⁶

Films assembled in the presence of lithium triflate (LiCF₃SO₃) were also investigated for sulfur, from which the atomic lithium content was estimated. For example, (PEO/PAA)_{LiTrif} multilayers assembled at pH 2.5 contained 0.78 wt % sulfur, yielding an atomic lithium content of 0.17 ± 0.06 wt %. For (PEO/PAA)_{LiTrif} multilayers, it was estimated that LbL films assembled at pH 2–3 contain 0.1–0.3 wt % lithium (Figure 4 of the Supporting Information), which roughly corresponds to EO:Li ratios of 13:1 to 28:1 (i.e., very low).

Electrochemical Impedance Spectroscopy. First studies⁴¹ of conductivity within electrostatic LbL assemblies suggested that ion transport within multilayers was enhanced in hydrophilic LbL interiors and humid (plasticized) conditions. In light of the previous assessment, the ionic conductivity of hydrogen-bonded multilayers with and without added salt is expected to reflect changes in assembly pH, salt content, and plasticization. Previous work by DeLongchamp et al. focused on (PEO/PAA) films constructed at a single pH (2.5), where a maximum conductivity of 1.3×10^{-5} S cm^{−1} (52% relative humidity, 25 °C, 1.0 M added salt) was reported.¹² Dry conductivities

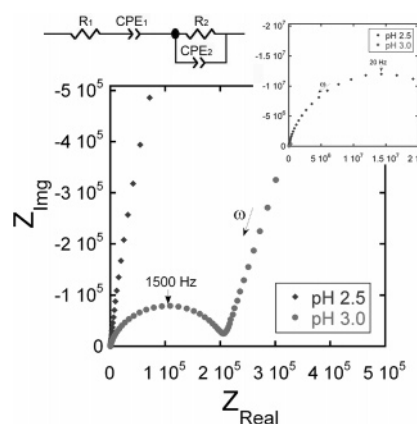


Figure 8. Nyquist plot (expanded axes are inset) of neat (PEO/PAA) and (PEO/PAA)_{LiTrif} multilayers (both assembled at pH 3) in a dry, argon-filled glovebox at 35 °C. The cell consisted of 30 layer pairs of LbL film sandwiched between blocking electrodes, ITO and Au. Voltage amplitude was 100 mV, and frequency range was 5 MHz to 0.1 Hz.

ranged from 10^{-12} to 10^{-10} S cm^{−1}, where the low conductivity was attributed to a high (but at that time unknown) glass transition temperature, hydrogen-bond cross-links, and poor segmental motion.¹² Here, changes in composition, T_g , and intermolecular hydrogen bonding (observed via FTIR and DSC) are expected to influence ionic mobility and charge carrier concentration, ultimately affecting ionic conductivity.

Electrochemical impedance spectroscopy was performed on LbL films (30 layer pairs, 2–4 μm thick) assembled at pH 2–3 with or without lithium triflate in a dry, argon-filled glovebox using an ITO|LbL|Au cell (see Supporting Information). PEO is known to conduct ions via a “rocking-chair” mechanism, where the alkali lithium cation is readily solvated by the ether oxygen and segmental motion and local relaxations aid in mobility.⁴² Conductivity from PAA is attributed to protons via dissociation (though limited in dry conditions)¹² or cations via counterion hopping (though limited when PAA is fully protonated). In a (PEO/PAA) LbL film, ionic conductivity is expected to be primarily a result of cation interaction with and mobility within PEO.

Both neat and lithium triflate systems exhibited a similar impedance response or Nyquist plot (Figure 8, assembly pH 3.00). At high frequencies, a depressed semicircle was observed; at low frequencies, a slanted near-vertical line was sometimes observed. Systems with higher impedance (less conductive) did not display the low-frequency vertical line because the impedance response of the system exceeded the limits of the analyzer. The observed response may be modeled by an equivalent circuit^{43,44} consisting of a resistor (R_1) and constant phase element (CPE_1) in series, followed by a resistor (R_2) and constant phase element (CPE_2) in parallel (Figure 8). Here, R_1 is considered the resistance of the blocking electrodes and wires, CPE_1 is a nonideal double layer, R_2 is the resistance of the LbL film, and CPE_2 describes bulk polarization of the LbL film. The conductivity of the system is calculated using $\sigma = L/(R_2A)$, where L is the thickness of the LbL film and A is the active area (6 mm²).

The dry (0% RH) conductivity of neat (PEO/PAA) multilayers assembled at pH 2–3 was 10^{-10} to almost 10^{-9} S cm^{−1} (Figure 9), and maximum conductivity detected was $(9 \pm 3) \times 10^{-10}$ S cm^{−1} for an LbL film of neat (PEO/PAA) assembled at pH 2.75. In this system, the charge carrier is believed to be residual ions (from assembly pH adjustment) or protons. The general increase in conductivity, when assembly pH varies from

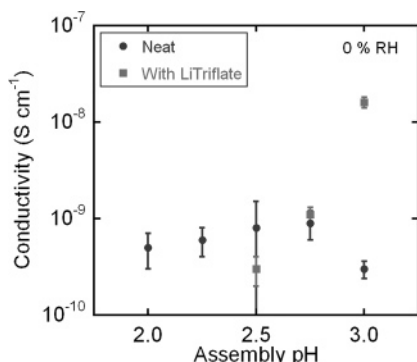


Figure 9. Ionic conductivity of neat (PEO/PAA) and (PEO/PAA)_{LiTrif} multilayers of varying assembly pH measured at 0% RH and 35 °C. The ionic conductivity was estimated from R_2 in the equivalent circuit described above. Measurements were performed in a dry, argon glovebox.

2 to 2.75, may be attributed to the inclusion of more amorphous PEO within the LbL film. From DSC, T_g decreases with increasing assembly pH; thus, PEO content increases with increasing assembly pH. Also, conductivities reported here (measured at ~ 35 °C) were higher than DeLongchamp's neat film of (PEO/PAA) assembled at pH 2.5, (4×10^{-11} S cm $^{-1}$ at 25 °C).¹² This discrepancy may be explained by the measurement conditions, where elevated temperature increases conductivity via either an Arrhenius or a Vogel–Tamman–Fulcher relationship.⁴²

The dry conductivity of (PEO/PAA)_{LiTrif} assemblies was also investigated (Figure 9). Conductivity ranged from below 10^{-9} to above 10^{-8} S cm $^{-1}$ as pH ranged from 2.5 to 3.0. Maximum conductivity was $(1.6 \pm 0.2) \times 10^{-8}$ S cm $^{-1}$ at pH 3 and 35 °C. Here, conductivity increases with pH, even though the observed glass transition temperature (via DSC) remains relatively invariant. One explanation may be that the charge carrier (Li^+) concentration increases with assembly pH, though this hypothesis was not conclusively verified via elemental analysis.

In comparison, solution-cast blends of PEO and lithium triflate of ether to lithium ratios similar to (PEO/PAA)_{LiTrif} films (13:1 to 28:1) demonstrate dry room-temperature conductivities slightly above $\sim 10^{-7}$ S cm $^{-1}$,⁴⁰ which is 10 times higher than the maximum conductivity of (PEO/PAA)_{LiTrif} assemblies, $\sim 10^{-8}$ S cm $^{-1}$. This difference suggests that the presence of PAA within the film may “dilute” the conductive media (PEO), thus increasing T_g and lowering the conductivity.

The impedance response of both systems was also investigated in a humidity-controlled box maintained at 53% RH, where LbL films absorb water, which acts as a plasticizer, from the humid environment.⁴⁵ In this case, the impedance response was similar to measurements performed in the dry state and could be modeled using the same equivalent circuit. The calculated conductivities (Figure 10) were measured with varying assembly pH for neat (PEO/PAA) and (PEO/PAA)_{LiTrif} systems. Results demonstrate that at pH 3.0 assembly conditions (PEO/PAA)_{LiTrif} LbL films are 100 times more conductive than neat (PEO/PAA) LbL films (10^{-7} vs 10^{-9} S cm $^{-1}$, respectively) at 53% RH and that conductivity appears to be independent of assembly pH.

The differences observed between the two systems at 0% and 53% RH are explained by the relationship $\sigma = nqu$,⁴² where σ is ionic conductivity, n is the number of charge carriers, q is electronic charge, and u is the mobility of the charge carriers. For example, adding lithium triflate to each assembly solution increases n so ionic conductivity is expected to increase. Neat

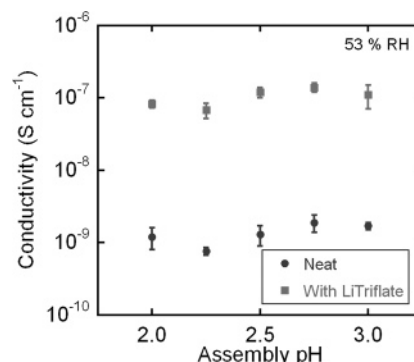


Figure 10. Ionic conductivity of neat (PEO/PAA) and (PEO/PAA)_{LiTrif} multilayers of varying assembly pH measured at 53% RH and 25 °C. Measurements were performed in a humidity-controlled vessel using magnesium nitrate hexahydrate. The ionic conductivity was estimated from R_2 in the equivalent circuit described above.

(PEO/PAA) LbL films contain few, if any, free ions (no ash left in elemental analysis), whereas (PEO/PAA)_{LiTrif} LbL films contained 0.1–0.3 wt % atomic lithium. At 53% RH, the influence of charge carrier concentration is clearly evident, where (PEO/PAA)_{LiTrif} multilayers are 100 times more conductive; at 0% RH, the effect of charge carrier concentration on ionic conductivity is not observed until assembly pH is above 2.75. The presence of water (humidity) increases μ and promotes local relaxations and segmental motion that are key to increasing ionic conductivity. Together, an LbL film that is both plasticized (via water) and doped (via LiCF_3SO_3) will yield a conductivity that is 100–1000 times higher (depending upon assembly pH) than its dry and undoped counterpart. For example, the conductivity of neat (PEO/PAA) at 0% RH was 3×10^{-10} S cm $^{-1}$, and that of (PEO/PAA)_{LiTrif} at 53% RH was 1.1×10^{-7} S cm $^{-1}$, each assembled at pH 3.00. Figures 5 and 6 of the Supporting Information describe the EIS humidity response of neat (PEO/PAA) and (PEO/PAA)_{LiTrif} multilayers.

In general, conductivity did not vary appreciably with assembly pH. One possible explanation is that the extent of hydrogen-bonding interactions, high enough to yield a stable LbL film, causes the film to behave as a cross-linked matrix where polymer backbones are essentially “pinned down”. Also, observed conductivity was below that of solution-cast PEO mixed with lithium triflate (10^{-6} S cm $^{-1}$);^{20,21} this difference is probably caused by the presence of PAA (which essentially dilutes the conductive medium and acts as a charge trap), poor segmental motion of the LbL film (high T_g), and the low concentration of carrier ions. Suggested means of improving conductivity in dry LbL films are (i) increasing the concentration of added salt within each bath or adding salt after assembly (increasing charge carrier concentration),¹² (ii) adding a liquid plasticizer (lowering T_g , increasing μ), and (iii) increasing PEO content.

A preliminary attempt to improve the dry-state conductivity included soaking a (PEO/PAA)_{LiTrif} LbL film, assembled at pH 3.0, in 0.1 M lithium hexafluorophosphate in propylene carbonate (LiPF_6/PC). This combination was chosen as a strategy to enhance performance via added salt and increased plasticization. Conductivity increased from $(1.6 \pm 0.2) \times 10^{-8}$ S cm $^{-1}$ for an untreated film to $(1.5 \pm 0.2) \times 10^{-7}$ S cm $^{-1}$ for a film soaked in LiPF_6/PC for 24 h, a 10-fold improvement.

A similar preliminary investigation was conducted for neat (PEO/PAA) LbL films, assembled at pH 3. Following a 24 h soak in LiPF_6/PC , dry-state conductivity increased from $(3.0 \pm 0.6) \times 10^{-10}$ to $(2 \pm 1) \times 10^{-6}$ S cm $^{-1}$, a 10000-fold improvement. The large improvement is attributed to the

inclusion of LiPF_6 within the film from the soaking solution and plasticization from PC. Of note, the conductivity of soaked neat (PEO/PAA) LbL films was 10 times greater than soaked (PEO/PAA) $_{\text{LiTrif}}$ films (10^{-6} vs 10^{-7} S cm^{-1} , respectively). One hypothesis for this difference is that neat (PEO/PAA) films contain substantially more PEO than (PEO/PAA) $_{\text{LiTrif}}$ films at assembly pH 3.0. Qualitatively, free-standing films of both systems, treated with LiPF_6/PC , were flexible, cohesive, and elastic.

Conclusion

In this work, the nature of hydrogen-bonding interactions within neat (PEO/PAA) multilayers was compared to those of films assembled in the presence of 0.1 M lithium triflate at a range of assembly pH. (PEO/PAA) $_{\text{LiTrif}}$ multilayer cycle thickness was greater than neat (PEO/PAA) films, an indication of suppressed acid–ether hydrogen-bonding interactions in the presence of added salt. From FTIR spectroscopy, 12–15% of PAA monomer units participated in intermolecular hydrogen bonding within (PEO/PAA) $_{\text{LiTrif}}$ multilayers, independent of assembly pH; in neat (PEO/PAA) multilayers, intermolecular hydrogen bonding increases with assembly pH (27% at pH 2 and 51% at pH 3). This implied that for neat (PEO/PAA) multilayers the PEO composition will increase with assembly pH; for (PEO/PAA) $_{\text{LiTrif}}$ systems, the PEO composition is expected to remain invariant. In terms of thermal properties, the glass transition temperature reflected the composition of the multilayer system. The T_g of neat (PEO/PAA) films decreased with increasing pH (59 °C at pH 2 and 26 °C at pH 3), whereas the glass transition temperature of (PEO/PAA) $_{\text{LiTrif}}$ multilayers was relatively invariant with pH (~48 °C). Together, these results suggest that intermolecular hydrogen bonding is suppressed during multilayer assembly in the presence of lithium triflate, whereas the dimerization of PAA is promoted. Because fewer carboxylic acid groups are available for hydrogen bonding with PEO, the film becomes enriched with PAA and the glass transition temperature increases. The lack of pH dependency (from pH 2 to 3) in (PEO/PAA) $_{\text{LiTrif}}$ multilayers indicates that the presence of 0.1 M salt screens the effect of assembly pH. Using electrochemical impedance spectroscopy, ionic conductivity was found to increase with increasing humidity (increasing mobility) and salt content (increasing charge carrier concentration). (PEO/PAA) $_{\text{LiTrif}}$ multilayers possessed an ionic conductivity of $\sim 10^{-7}$ S cm^{-1} at 53% RH, and dry, neat (PEO/PAA) multilayers were 10^{-10} – 10^{-9} S cm^{-1} . Increasing assembly pH appeared to increase the dry, 0% humidity, conductivity of both neat and lithium triflate (PEO/PAA) systems. In the case of neat (PEO/PAA) multilayers, the dry conductivity is thought to increase with assembly pH because of the increasing PEO content (evidenced by decreasing T_g) in the case of (PEO/PAA) $_{\text{LiTrif}}$ multilayers, the increase is possibly attributed to increasing charge carrier concentration. Dry-state conductivities reaching 10^{-6} S cm^{-1} are possible for (PEO/PAA) LbL systems soaked in 0.1 M lithium hexafluorophosphate and propylene carbonate, which are believed to dope and plasticize the LbL matrix.

Acknowledgment. We thank the Dupont-MIT Alliance and the Institute of Soldier Nanotechnology for funding as well as the Center for Materials Science and Engineering for facilities. J.L. thanks the National Science Foundation Graduate Fellowship.

Supporting Information Available: Experimental, materials, and methods; FTIR spectra of COOH region; sample DSC curve; elemental analysis; EIS and Nyquist plots of neat and salt-added (PEO/PAA) multilayers at varying humidity. This material is available free of charge via the Internet at <http://pubs.acs.org>.

References and Notes

- (1) Bekturov, E. A.; Bimendina, L. A. *Adv. Polym. Sci.* **1981**, *41*, 100–147.
- (2) Tsuchida, E.; Abe, K. *Adv. Polym. Sci.* **1982**, *45*, 1–125.
- (3) Tsuchida, E.; Takeoka, S. Interpolymer Complexes and Their Ion-Conduction. In *Macromolecular Complexes in Chemistry and Biology*; Dubin, P., Bock, J., Davis, R., Schulz, D. N., Thies, C., Eds.; Springer: Berlin, 1994; pp 183–213.
- (4) Stockton, W. B.; Rubner, M. F. *Macromolecules* **1997**, *30*, 2717–2725.
- (5) Wang, L.; Wang, Z.; Zhang, X.; Shen, J.; Chi, L.; Fuchs, H. *Macromol. Rapid Commun.* **1997**, *18*, 509–514.
- (6) Kharlampieva, E.; Sukhishvili, S. A. *J. Macromol. Sci., Part C: Polym. Rev.* **2006**, *46*, 377–395.
- (7) Wang, L.; Fu, Y.; Zhiqiang, W.; Yuguo, F.; Zhang, X. *Langmuir* **1999**, *15*, 1360–1363.
- (8) Baranovsky, V. Y.; Litmanovich, A. A.; Papisov, I. M.; Kabanov, V. A. *Eur. Polym. J.* **1981**, *17*, 969–979.
- (9) Decher, G. *Science* **1997**, *277*, 1232–1237.
- (10) Lutkenhaus, J. L.; Hrabak, K. D.; McEnnis, K.; Hammond, P. T. *J. Am. Chem. Soc.* **2005**, *127*, 17228–17234.
- (11) Sukhishvili, S. A.; Kharlampieva, E.; Izumrudov, V. *Macromolecules* **2006**, *39*, 8873–8881.
- (12) DeLongchamp, D. M.; Hammond, P. T. *Langmuir* **2004**, *20*, 5403–5411.
- (13) Sukhishvili, S. A.; Granick, S. *Macromolecules* **2002**, *35*, 301–310.
- (14) Kozlovskaya, V.; Sukhishvili, S. A. *Macromolecules* **2006**, *39*, 5569–5572.
- (15) Kozlovskaya, V.; Ok, S.; Sousa, A.; Libera, M.; Sukhishvili, S. A. *Macromolecules* **2003**, *36*, 8590–8592.
- (16) Sukhishvili, S. A.; Granick, S. *J. Am. Chem. Soc.* **2000**, *122*, 9550–9551.
- (17) Zhang, X.; Chen, H.; Zhang, H. *Chem. Commun.* **2007**, 1395–1405.
- (18) Zhang, H.; Fu, Y.; Wang, D.; Wang, L.; Wang, Z.; Zhang, X. *Langmuir* **2003**, *19*, 8497–9502.
- (19) Bai, S.; Wang, Z.; Zhang, X. *Langmuir* **2004**, *20*, 11828–11832.
- (20) Wiczeorek, W.; Raducha, D.; Zalewska, A.; Stevens, J. R. *J. Phys. Chem. B* **1998**, *102*, 8725–8731.
- (21) Tarascon, J.-M.; Armand, M. *Nature (London)* **2001**, *414*, 359–367.
- (22) Seo, J.; Lutkenhaus, J. L.; Kim, J.; Hammond, P. T.; Char, K. *Macromolecules* **2007**, *40*, 4028–4036.
- (23) Clark, S. L.; Montague, M. F.; Hammond, P. T. *Macromolecules* **1997**, *30*, 7237–7244.
- (24) Shiratori, S.; Rubner, M. F. *Macromolecules* **2000**, *33*, 4213–4219.
- (25) Choi, J.; Rubner, M. F. *Macromolecules* **2005**, *38*, 116–124.
- (26) Bailey, F. E.; Koleske, J. V. *Poly(ethylene oxide)*; Academic Press: New York, 1976; pp 87–118.
- (27) Painter, P. C.; Brozoski, B. A.; Coleman, M. M. *J. Polym. Sci., Polym. Phys. Ed.* **1982**, *20*, 1069–1080.
- (28) Lu, X.; Weiss, R. A. *Macromolecules* **1995**, *28*, 3022–3029.
- (29) Bellamy, L. J. *The Infra-red Spectra of Complex Molecules*; Chapman and Hall: London, 1975; pp 183–200.
- (30) Nishi, S.; Kotaka, T. *Macromolecules* **1985**, *18*, 1519–1525.
- (31) Lee, J. Y.; Painter, P. C.; Coleman, M. M. *Macromolecules* **1988**, *21*, 346–364.
- (32) Teeters, D.; Neuman, R. G.; Tate, B. D. *Solid State Ionics* **1996**, *85*, 239–245.
- (33) Lee, J. Y.; Painter, P. C.; Coleman, M. M. *Macromolecules* **1988**, *21*, 954–960.
- (34) Coleman, M. M.; Lee, J. Y.; Serman, C. J.; Wang, Z.; Painter, P. C. *Polymer* **1989**, *30*, 1298–1307.
- (35) Han, K.; Williams, L. J. *J. Appl. Polym. Sci.* **1991**, *42*, 1845–1859.
- (36) Bailey, F. E.; Lundberg, R. D.; Callard, R. W. *J. Polym. Sci., Part A* **1964**, *2*, 845–851.
- (37) Smith, K. L.; Winslow, A. E.; Petersen, D. E. *Ind. Eng. Chem.* **1959**, *51*, 1361–1364.
- (38) Hoffmann, H.; Liveri, M. L. T.; Cavasino, F. P. *J. Chem. Soc., Faraday Trans.* **1997**, *93*, 3161–3165.
- (39) Fox, T. G. *Bull. Am. Phys. Soc.* **1956**, *1*, 123.
- (40) Boileau, S.; Bouteiller, L.; Foucat, E.; Lacoudre, N. *J. Mater. Chem.* **2002**, *12*, 195–199.
- (41) Durstock, M. F.; Rubner, M. F. *Langmuir* **2001**, *17*, 7865–7872.
- (42) Gray, F. M. *Polymer Electrolytes*; Royal Society of Chemistry: Cambridge, 1997; p 175.
- (43) Bruce, P. G. In *Polymer Electrolyte Reviews*; MacCallum, J. R., Vincent, C. A., Eds.; Elsevier Applied Science Publishers: London, 1996; pp 237–274.
- (44) DeLongchamp, D. M.; Hammond, P. T. *Chem. Mater.* **2003**, *15*, 1165–1173.
- (45) Smith, A. L.; Ashcraft, J. N.; Hammond, P. T. *Thermochim. Acta* **2006**, *450*, 118–125.